An integrated model of fixational eye movements and microsaccades

Ralf Engbert[a,1], Konstantin Mergenthaler[a,2], Petra Sinn[a], and Arkady Pikovsky[b]

Departments of [a]Psychology and [b]Physics, University of Potsdam, 14469 Potsdam, Germany

Edited by Dale Purves, Duke University Medical Center, Durham, NC, and approved August 3, 2011 (received for review February 18, 2011)

When we fixate a stationary target, our eyes generate miniature (or fixational) eye movements involuntarily. These fixational eye movements are classified as slow components (physiological drift, tremor) and microsaccades, which represent rapid, small-amplitude movements. Here we propose an integrated mathematical model for the generation of slow fixational eye movements and microsaccades. The model is based on the concept of self-avoiding random walks in a potential, a process driven by a self-generated activation field. The self-avoiding walk generates persistent movements on a short timescale, whereas, on a longer timescale, the potential produces antipersistent motions that keep the eye close to an intended fixation position. We introduce microsaccades as fast movements triggered by critical activation values. As a consequence, both slow movements and microsaccades follow the same law of motion; i.e., movements are driven by the self-generated activation field. Thus, the model contributes a unified explanation of why it has been a long-standing problem to separate slow movements and microsaccades with respect to their motion-generating principles. We conclude that the concept of a self-avoiding random walk captures fundamental properties of fixational eye movements and provides a coherent theoretical framework for two physiologically distinct movement types.

The human visual system is highly adaptive to constant input, which can induce perceptual fading of stationary scenes. This fact has been demonstrated by laboratory experiments during which an image was perfectly stabilized on the retina (1, 2). Although such a visual system might be optimized for the detection of approaching predators or escaping prey, a detailed analysis of stationary objects is precluded because of rapid perceptual fading due to neural adaptation (3). Therefore, paradoxically, our eyes must generate miniature (or fixational) eye movements to refresh the input of the retinal receptor systems continuously (4–6). Under normal, head unrestrained viewing conditions, body and head movements might help to prevent image fading; however, statistical properties of postural fluctuations and miniature eye movements are qualitatively different (7). If these statistical differences are functional, then postural fluctuations could not replace fixational eye movements.

Three physiological components of fixational eye movements are distinguished: drift, tremor, and microsaccades (8). Drift and tremor (oscillatory components of fixational eye movements) are slow movements with small amplitudes, whereas microsaccades represent a ballistic component of fixational eye movements (Fig. 1). As a consequence, microsaccades are characterized as roughly linear movement epochs with durations up to 30 ms and a frequency of one to two per second.

It was discovered in the 1960s that microsaccades share kinematic properties, e.g., a fixed relation between amplitude and peak velocity, with inspection saccades observed during free viewing or reading (9). Among the long-standing research problems in vision was the question of whether it is possible to find a specific function for microsaccades (4). For example, it was demonstrated (10) that slow movements (drift) are sufficient to keep the eye at this intended fixation position. After considerable discussion (11), some researchers concluded that microsaccades "serve no useful purpose" (ref. 12, p. 273).

Over the last 10 y, progress has been made in the study of the role of microsaccades for vision (8, 13). Among the numerous findings on fixational eye movements and microsaccades, it was demonstrated that microsaccades induce enhanced neural activity (bursting) across the visual pathway (14, 15) as well as decreased neural activity (16–18). Moreover, microsaccades are coupled to visual attention (19, 20), and fixational eye movements in general are critical to high-acuity vision (21–23). Furthermore, it could be demonstrated that microsaccades play a role in second-order visibility, because they counteract filling in of artificial scotomas (24).

Using different experimental manipulations of visibility, it could be shown that image fading did not trigger a direct response by the generation of microsaccades (25), although this finding does not rule out a role for microsaccades in the prevention of perceptual fading. However, Martinez-Conde et al. (21) observed that microsaccade production counteracted perceptual fading and induced target visibility during fixation. On the basis of similar findings that underline the complicated relationship between microsaccades and vision, it was concluded in a recent review (ref. 26, p. 1) that "there is no compelling evidence to support the view that microsaccades [. . .] serve a necessary role in improving oculomotor control or in keeping the visual world visible." Such a conclusion challenges the view that microsaccades have a specific function for vision (8) compared to slow components of fixational eye movements. Using computational modeling, we study possible theoretical reasons for the difficulty in finding a specific motion-generating principle for microsaccades.

Are microsaccades and saccades different processes? On the one hand, kinematic analyses and studies on the role of visual attention for microsaccades emphasize the similarity between microsaccades and saccades in fixation tasks (27) as well as in natural viewing tasks (28). On the other hand, microsaccades are tightly coupled to the drift component of fixational eye movements. For example, the drift component of fixational eye movements tends to be slower before a microsaccade than when no microsaccade is generated (29). Moreover, we suggested previously (5) that the generating process for microsaccades is a Poisson process; i.e., microsaccades are generated with a constant rate over time, indicated by an exponential intermicrosaccade interval (IMSI) distribution (5, 30). However, in an earlier study (28) no such difference was observed. Therefore, whereas some properties of microsaccades suggest that microsaccades are a microscopic

Author contributions: R.E. and A.P. designed research; R.E. and K.M. performed research; R.E., K.M., and P.S. analyzed data; and R.E. wrote the paper.

The authors declare no conflict of interest.

This article is a PNAS Direct Submission.

Freely available online through the PNAS open access option.

[1]To whom correspondence should be addressed. E-mail: Ralf.Engbert@uni-potsdam.de.

[2]Present address: Department of Software Engineering and Theoretical Computer Science, Technische Universität Berlin, Straße des 17. Juni 135, 10623 Berlin, Germany.

See Author Summary on page 16149.

This article contains supporting information online at www.pnas.org/lookup/suppl/doi:10.1073/pnas.1102730108/-/DCSupplemental.

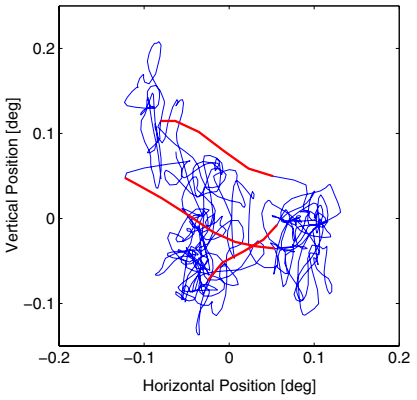

Fig. 1. Fixational eye movements and microsaccades. Data were recorded from fixational eye movements during a fixation of 2 s. Slow movements (blue) are highly erratic, whereas microsaccades (red) are ballistic, small-amplitude epochs with a more linear trajectory (compared with the slow background motions). The sample trajectory was recorded with a sampling frequency of 500 Hz (for details see ref. 29).

counterpart of saccades, analyses of the generating process motivated our hypothesis that microsaccades are dynamically linked to slow components of fixational eye movements and might be described by an integrated model.

Recent advances in mathematical modeling of fixational eye movements and microsaccades focused on visual function (31–33). Here we suggest a set of mechanisms for the potential generating processes of miniature eye movements and develop an integrated model of fixational eye movements and microsaccades. The starting point for our mathematical model of fixational eye movements is the experimental observation of a highly specific correlation structure with a transition from persistent behavior (i.e., the statistical tendency of a random walk to maintain its current movement direction) on a short timescale to antipersistent behavior (i.e., the tendency to reverse its current direction) on a longer timescale (34–36). This characteristic correlation pattern can be explained by a self-avoiding random walk (37) in a potential. We show that this concept provides a coherent framework for several properties of fixational eye movements and that it can be extended to include a generating mechanism for microsaccades.

We must clarify, however, that our model is based on data recorded with video-based eye trackers, in which one component of the measured slow eye movements could be masked by pupil-diameter fluctuation artifacts (38).

Mathematical Model

We develop our model in several steps. We propose a mathematical model of a self-avoiding random walk in a potential that reproduces the temporal correlations observed in fixational eye movements. After we demonstrate the viability of our approach using numerical simulations, we suggest a mechanism for the generation of microsaccades within the same theoretical framework.

Self-Avoiding Random Walk. Although it is traditionally thought that fixational eye movements represent noise in the oculomotor system (39), recent studies demonstrated that a characteristic correlation pattern can be found in the eye's random walk during fixation. Our model is mainly motivated by the observation that fixational eye movements are persistent on a short timescale (34); i.e., the eye exhibits the statistical tendency to continue to travel in its current movement direction. Therefore, as a conceptual model of fixational eye movements, it seems promising to implement a random walk that avoids moving to regions of space that were visited shortly before, i.e., a self-avoiding walk. In 1992, a specific model for a self-avoiding walk on a lattice was proposed by Freund and Grassberger (37), which we use as a starting point for our model.

Let us consider a random walker on a finite square lattice of size $L \times L$ with periodic boundary conditions. Freund and Grassberger (37) were inspired by a phenomenology of a walk in a swamp, where the ground under a walker located at lattice site (i, j) sinks,

$$h_{ij} \to h_{ij} + 1. \quad [1]$$

Here activation h_{ij} represents the ground depth at site (i, j). All nonoccupied sites (k, l) different from (i, j) relax back to the steady zero level according to a law

$$h_{kl} \to (1 - \varepsilon) \cdot h_{kl}. \quad [2]$$

This is a special case of a more general relation used in the original work (37): Our choice is a linear relaxation law in Eq. **2**. The parameter ε is called the relaxation rate of the activation field. The numerical value of ε will turn out to be critical for the observation of persistent behavior.

The random walk is governed by the iteration rule to take a step from site (i, j) to that site among the four neighboring sites $\{(i-1, j), (i+1, j), (i, j-1), (i, j+1)\}$ with the smallest activation $h_{\cdot}$. If two (or more) of the adjoined sites display the same (minimal) value of the activation, then a random site among this set of neighbors is chosen with equal probability. Following Freund and Grassberger (37), it is important to note that the random walk is completely determined by a shortsighted rule; i.e., no long-term strategy is used, and the decision on the next step is based only on the value of the activation at the current site and the activation of the four neighbors. As a result, the walker tries to avoid returning to recently visited sites and a self-organized distribution of activation over the lattice is built up.

The activation field in our model is neurophysiologically plausible. We interpret the value h_{ij} as the activation of neuron (i, j) in the motor map of the superior colliculus, the top-level brainstem structure controlling saccadic eye movements (40, 41). Such a hypothetical activation (27) could serve as a neurophysiological mechanism (42) to implement a self-avoiding walk.

Self-Avoiding Walk in a Potential. Because fixational eye movements are confined to a small area, the foveal region representing ~2° of visual angle, we studied the self-avoiding walk in a 2D, quadratic potential; i.e.,

$$u(i,j) = \lambda L \left(\left(\frac{i - i_0}{i_0} \right)^2 + \left(\frac{j - j_0}{j_0} \right)^2 \right), \quad [3]$$

where the site (i_0, j_0) represents the center of the lattice. The site (i_0, j_0) is interpreted as the rostral pole of the superior colliculus related to movements with vanishing amplitudes (41, 42). The new iteration rule for the self-avoiding walk in a potential requires that the walker always moves to the minimum of the sum of the activation and the potential across the four neighboring sites with position

$$(i', j') = \underset{(k,l) \in N(i,j)}{\arg\min} \{h_{kl} + u(k,l)\}, \quad [4]$$

where $N(i, j) = \{(k, l) \mid k = i \pm 1 \text{ and } l = j \pm 1\}$.

Next, we carried out numerical simulations (*i*) to investigate the statistical properties of the model and (*ii*) to include the generation of microsaccades within the framework of a self-avoiding random walk.

Results

Basic Statistical Properties of the Model. Our numerical simulations were performed on a $L \times L$ lattice with a linear dimension $L = 51$. The center of the potential $u(i, j)$ was given by $i_0 = j_0 = (L-1)/2 = 25$. The slope parameter λ was chosen as $\lambda = 1$. To observe persistent behavior despite the restoring force resulting from the potential, a very slow relaxation rate $\varepsilon = 10^{-3}$ of the activation field $\{h_{ij}\}$ was necessary. The simulations were started at a random lattice site. To remove transients, we run the model for 10,000 iterations. A typical trajectory of the resulting random walk is illustrated in Fig. 2*A*, where noise was added to the lattice points after the simulation for the illustration of the trajectory. The highlighted first 50 simulated data points demonstrate that the walker locally avoids intersecting its own trajectory, whereas the potential controls the overall mean position of the walker, i.e., the intended fixation position.

For a quantitative analysis of correlations on short and long timescales of the random walk generated by our model, we estimated the mean square displacement of the random walk at a lag l between two iterations x_{i-l} and x_i (34, 43),

$$D^2(l) = \frac{1}{2(N-l)} \sum_{i=1}^{N-l} \|\vec{x}_{i-l} - \vec{x}_i\|^2. \quad [5]$$

In fixational eye movement data, a plot of the mean square displacement $D^2(l)$ as a function of the lag l indicated power-law behavior; i.e.,

$$D^2(l) \propto l^{\alpha}, \quad [6]$$

where α is the scaling exponent. Experimentally, fixational eye movements show persistence, i.e., $\alpha_s > 1$ on a short timescale with $l < 20$ ms, and antipersistence, i.e., $\alpha_l < 1$ on a longer timescale $l > 100$ ms (34). These findings were checked with surrogate data (34) and replicated using detrended fluctuation analysis (DFA) (35, 36) as an advanced technique to verify the existence of long-range correlations.

The analysis of the mean square displacement of simulated trajectories demonstrated that our self-avoiding random walk in a quadratic potential reproduced the experimentally observed transition from persistence to antipersistence (Fig. 2*B*). We fitted two linear regressions in the double-logarithmic representation of Fig. 2*B*. The scaling exponent $\alpha_s = 1.32 \pm 0.02$ indicated persistence on a short timescale, $l \leq 10$ iterations. The corresponding simulated result is in good agreement with the experimentally observed value of $\alpha_s^{(exp)} = 1.38 \pm 0.05$ (34). In the simulations, antipersistence with $\alpha_l = 0.71 \pm 0.06$ was reproduced on a longer timescale, $10 \leq l \leq 50$ iterations; again, there is agreement with the experimental result, $\alpha_l^{(exp)} = 0.79 \pm 0.11$. Therefore, our model captured the characteristic transition from persistence to antipersistence found in experimental data on fixational eye movements and generated numerically reasonable approximations for the scaling exponents.

Note that the data basis (34) for our model was obtained from a video-based eye tracker. Although simple measurement noise cannot create the timescale separation observed in our data, pupil-size fluctuations could potentially introduce artifacts in slow eye movements (38). In the next section, we add a principle for the generation of microsaccades to our model.

A Mechanism for the Generation of Microsaccades. Although our model reproduced important statistical properties of fixational eye movements, it is incomplete with respect to the occurrence of microsaccades. Microsaccades are traditionally classified as a distinct type of fixational eye movements representing ballistic jumps with small amplitudes (<1°). In this section, we propose a generating mechanism that emerges from critical states of activation in our model.

During the iteration of the self-avoiding random walk (Fig. 2*A*), the walker generates an activation field $\{h_{ij}\}$, which gives a stationary distribution after transients have been removed. A corresponding snapshot of the activation field is plotted in Fig. 3*A*. The shape of the distribution is determined by the relaxation rate ε and the slope of the potential λ. We observed that for increasing λ, the distribution of the activation becomes more and more asymmetric. In Fig. 3*B*, the distributions are compared for three different values of λ. For small values ($\lambda = 0.15$ and 0.30) the distribution is approximately symmetric. However, for a larger value of the slope ($\lambda = 1.00$), the distribution is negatively skewed (skewness $s = -0.47$). We interpret this finding by postulating that the potential moves the walker against its statistical tendency to avoid lattice sites with high activations—the steeper the potential is, the more frequently the walker visits lattice sites with high activations.

Thus, the system self-organizes to a stationary distribution characterized by a mode toward the right tail (i.e., a distribution with negative skewness), which can be used to define a charac-

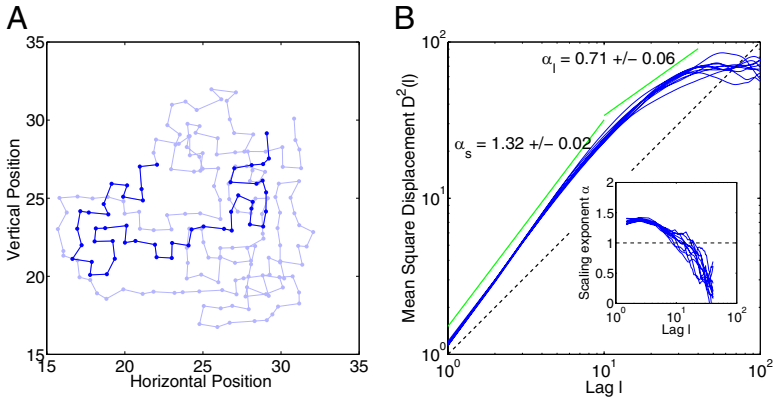

Fig. 2. Simulation of the self-avoiding random walk in a quadratic potential. (*A*) A sample trajectory with 1,000 iterations of the model (after removing transients). Lattice points are jittered by noise for visibility. The first 50 simulated data points are highlighted to demonstrate that the trajectory is self-avoiding on a short timescale; i.e., the trajectory does not intersect itself. (*B*) The model generates a transition from persistence to antipersistence. For uncorrelated random motions, a scaling exponent $\alpha = 1$ (dashed line) would be obtained for the mean square displacement. For the simulated data, we computed significantly different slopes (green lines indicate average slopes). The scaling exponent demonstrates persistent behavior ($\alpha_s > 1$) on a short timescale (lag $l < 10$ iterations) and antipersistent behavior ($\alpha_l < 1$) on a long timescale (lag $l > 10$ iterations), which is in good agreement with experimental results.

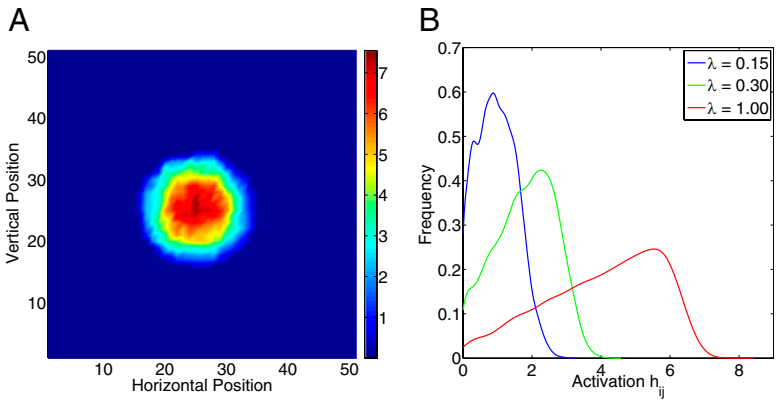

Fig. 3. Distribution of activation generated by the self-avoiding random walk. (*A*) The confinement of the walker due to the quadratic potential generates a unimodal stationary distribution over the activation field $\{h_{ij}\}$. (*B*) Distribution of the activations $\{h_{ij}\}$ as a function of the slope parameter λ of the potential. For increasing values of λ, the distributions self-organize toward an asymmetric form with a well-defined maximum value.

teristic (or critical) activation threshold for the generation of microsaccades. We assume that, if the walker moves to a site (i, j) with an activation h_{ij} higher than the critical threshold h_c, i.e., $h_{ij} > h_c$, then a microsaccade is triggered. The endpoint of the microsaccade is defined as the site (i', j') with the global minimum of the sum of activation field and potential corresponding to Eq. **4**, with $N = \{(i, j) \mid 1 \le i, j \le L\}$. In sum, if the walker reaches a site with activation greater than the critical activation, then a microsaccade is immediately initiated toward the site with the global minimum of activation.

Experimental data suggest that IMSIs are exponentially distributed; i.e., a Poisson process is a simple model for the generation of microsaccades (5, 29, 30). We carried out numerical simulations of our model with a critical value $h_c = 7.9$ of the threshold for triggering of microsaccades (Movie S1). The resulting distribution of IMSIs turned out to have an exponential form (Fig. 4). Thus, the model generates the experimentally observed exponential distribution of interevent times, which mimics a Poisson process, on the basis of the dynamic triggering mechanism.

Oculomotor Potential. For human observers, some experimental data show that the spatial orientation of microsaccades is characterized by a strong preference to horizontal and vertical movement vectors (5, 20). This preference might be related to the neural circuitry of the saccadic system, because different

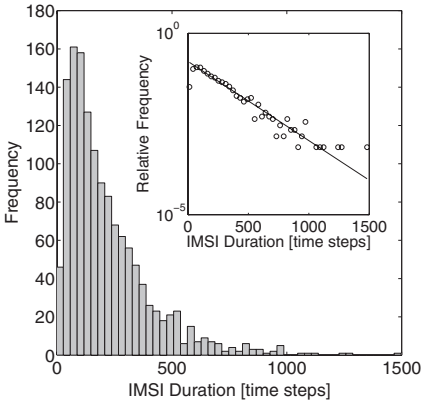

Fig. 4. Distribution of intermicrosaccadic intervals. The dynamic triggering mechanism for microsaccades reproduced the experimentally observed exponential distribution of interevent times (see linear fit of the semilogarithmic plot in the inset).

nuclei of the brainstem circuitry are controlling horizontal and vertical saccades (41). For voluntary saccades, a neural mechanism exists for the coordination of oblique orientations. At least for human participants, such a coordinating mechanism might be inactive in the case of microsaccades, which are characterized by low activation of the saccadic system (42).

To capture the preference for purely horizontal or vertical microsaccade orientations, we introduced an additional oculomotor potential of the form

$$u_1(i,j) = \chi L\left(\left(\frac{i-i_1}{i_0}\right)^2 \cdot \left(\frac{j-j_1}{j_0}\right)^2\right), \qquad [7]$$

defined with respect to lattice site (i_1, j_1), where the microsaccade is launched. For the selection of the microsaccadic endpoint (or landing site), we determined the global minimum of the sum of (*i*) the activation field h_{ij}, (*ii*) the quadratic potential $u(i, j)$, and (*iii*) the oculomotor potential $u_1(i, j)$, i.e., $\min_{(k,l)}\{h_{kl} + u(k, l) + u_1(k, l)\}$. As a result, the oculomotor potential forces the microsaccades to show the experimentally observed preference. For the numerical simulations, we fixed the slope parameter χ of the oculomotor potential, Eq. **7**, at a value of $\chi = 2\lambda = 2$. The resulting angular distribution of microsaccades is shown in Fig. 5.

The oculomotor potential was introduced to adjust the resulting distribution of orientations of microsaccades to the experimentally observed distribution in some studies. It is important to note that the problem of orientation preferences is not critical to our modeling assumptions. We checked with numerical simulations that the statistical properties of our model do not depend on the assumption of an oculomotor potential.

After the development of our model based on the three principles of (*i*) a self-avoiding random walk on a lattice in (*ii*) a 2D quadratic potential and with (*iii*) a mechanism for the generation of microsaccades and an additional oculomotor potential, we investigate the model's prediction on the relation between microsaccades and physiological drift in the next section.

Dynamical Interactions Between Microsaccades and Drift. Our mathematical model of the generation of fixational eye movements and microsaccades provides a coherent theoretical framework for the random component (physiological drift) and the ballistic component (microsaccades). As a critical test for our model, we now investigate whether our model can predict interactions between drift and microsaccades. Using data from a visual fixation task, it was shown that the drift component of fixational eye movements is slower before a microsaccade than when no such movement is generated (29). For such an analysis, the graph

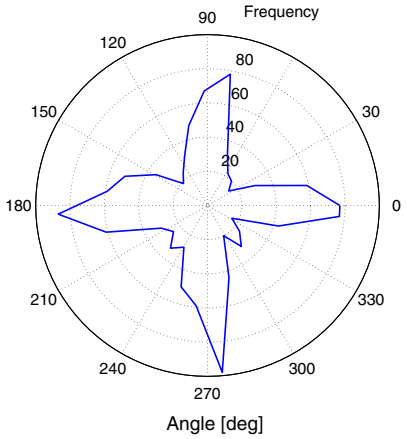

Fig. 5. Angular distribution of microsaccades. Due to the oculomotor potential u_1, microsaccades in the model reproduce the experimentally observed preference for purely horizontal or vertical movement vectors as observed in human microsaccade recordings.

of the eye's trajectory is covered by boxes of a linear dimension of $\Delta = 1$ lattice unit (Fig. 6*A*). Experimentally, a numerical value of $\Delta^{(\mathrm{exp})} = 0.01°$ was chosen (29), which corresponds to the approximate size of a retinal cone receptive field (44).

The number of boxes (or box count) needed to cover the trajectory over a time window of 20 iterations provides a geometric measure of movement activity. We performed the same analysis for the simulated data as for the experimental data (29), other than the fact that spatial and temporal scales are arbitrary in the simulations. As a result, a significant reduction of the precursory box count is observed before microsaccade onset (Fig. 6*B*), a result that mimics the interaction of drift and microsaccades observed from experimental data. We remark that these simulations confirm the existence of a dynamical coupling between drift and microsaccades; however, the model does not make any further claim on possible differences between microsaccades and small voluntary saccades.

Relation Between Precursory Box Count and Microsaccade Amplitude. We investigated the possible relation between the size of the precursory box count and the amplitude of the microsaccade that is generated at the end of the time window for the calculation of the box count. We computed the linear correlation coefficient for 150 runs of the model and obtained a negative slope with a mean value of –0.06 ($P < 0.001$). Therefore, the model makes the specific prediction that a higher amount of retinal image slip before a microsaccade will lead to a smaller microsaccade amplitude. To test this prediction experimentally, we carried out an analysis of data (experiment 2) from our earlier publication (29) on the retinal image slip before microsaccades. This analysis confirmed the model's prediction of a negative correlation. We obtained a significant slope of –0.05 ($P < 0.01$), when the box count was computed at a time lag of 300 ms before the microsaccade. Moreover, the slope value was numerically negative over a broad range of time lags from 200 ms to 500 ms before a microsaccade. Using this reanalysis of experimental data, we were able to find substantial support for a specific prediction of the mathematical model. Finally, in free-viewing tasks, top–down saccadic signals should not interfere with slow movements, except for preparatory motor activity immediately before the saccade. Compatible with such an expected absence of a dynamical coupling to epochs of physiological drift, we found a zero correlation in a scene-viewing paradigm (30).

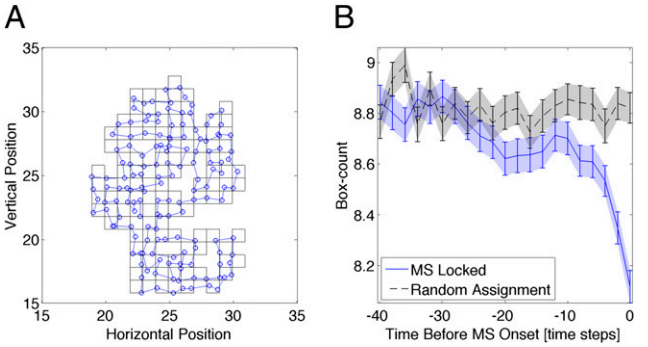

Fig. 6. Precursory box count computed from time windows immediately before microsaccades. (*A*) The simulated trajectory is covered by boxes of linear dimension $\Delta = 1$ lattice units to quantify the area visited by drift movements in a given time window. (*B*) The number of boxes needed to cover simulated data from a time window of 20 iterations indicates that microsaccades are preceded by reduced retinal image slip (blue, microsaccade-locked time windows). For the computation of the plot, time windows extended backward in time [e.g., box count for $t = -40$ computed from time window (–60; –40) and $t = 0$ computed from (–20; 0)]. In a statistical control (gray, random assignments), we selected random intervals without microsaccades and obtained an approximately constant box count.

Discussion

The aim of the current theoretical study was to formulate an integrated model of fixational eye movements and microsaccades. The model is based on the concept of self-avoiding random walks (37), which is a behaviorally important and physiologically plausible principle for fixational eye movements. To refresh the perceptual input to the retinal receptor systems, eye movements during fixation must perform small retinal image shifts continually (6, 8). An optimal strategy to serve this function is implemented by random motions, which, in a statistical sense, visit new regions of the visual field preferentially. Such a behavior is a built-in mechanism of self-avoiding random walks. At the same time, a self-avoiding walk can explain the persistent statistical correlations observed in fixational eye movements (34).

Because excursions of the eye's movements during fixation must stay within the foveal region of the visual field, we studied the self-avoiding walk in a potential. A potential might be interpreted as our voluntary strategy to fixate a current visual object for high-acuity analysis. The neurophysiological basis of such a potential is likely to be implemented by tonic units of the brainstem oculomotor circuitry (41). These neurons generate action potentials with a rate proportional to the eye's eccentricity. Both principles, the self-avoiding walk and the restoring forces due to the potential, generate a transition from persistence on short timescales to antipersistence on longer timescales, one of the fundamental statistical properties of fixational eye movements (34) and other physiological systems (43).

Next, we included microsaccades in our model by a threshold mechanism. Whenever the eye visits a lattice site with a critical activation, a microsaccade, i.e., a ballistic movement to the global minimum of activation, is initiated. Such a mechanism for the generation of microsaccades is based on only one additional model parameter, the critical activation h_c, and is psychologically and neurophysiologically plausible, because it is well established that microsaccades do only marginally contribute to the correction of small fixation errors (5, 6). In our model, this behavior is reproduced because the global minimum of activation (as a target for a microsaccade) can appear at arbitrary positions on the lattice and is not always located near the center of the potential. Recently, an interaction between subsequent microsaccade orientations was reported for high-acuity visual tasks like needle

threading (23). Our self-avoiding random-walk model, simulated in a double-well potential, might help to explain these interactions.

The model reproduced our earlier finding that retinal image motion (quantified by a box-count measure) is slower before microsaccades compared with drift epochs (29). Additionally, the model predicted a negative correlation between the size of the precursory box count and the microsaccade amplitude. This prediction was in good agreement with experimental data on microsaccades during a fixation task (29). As a result, there is experimental evidence for one of the model's core properties, i.e., the dynamical relation between physiological drift and microsaccades.

Our model proposes that microsaccades predominantly follow the same underlying laws of motion as physiological drift. Both types of movements are driven by a self-generated activation field, in addition to the fact that microsaccades exhibit different movement kinematics than slow components of fixational eye movements. Taken together, our model might help to explain why microsaccades can hardly be distinguished from ocular drift in terms of their motion-generating principle—a problem underlying the scientific dispute between Ditchburn (11) and Kowler and Steinman (12) ~30 y ago.

ACKNOWLEDGMENTS. We thank Elke B. Lange, Jochen Laubrock, and Hans A. Trukenbrod for comments on the manuscript. Portions of this research were presented at the Minerva-Weizmann Workshop on "Active Sensing in Touch, Vision, and Smell" on December 2–5, 2008, at the Weizmann Institute, Rehovot, Israel. We thank Ehud Ahissar for the invitation to the workshop and for valuable discussions. This work was funded by Deutsche Forschungsgemeinschaft Research Group 868 "Computational Modeling of Behavioral, Cognitive, and Neural Dynamics" Grant EN 471/3.

1. Ditchburn RW, Ginsborg BL (1952) Vision with a stabilized retinal image. *Nature* 170: 36–37.
2. Riggs LA, Ratliff F, Cornsweet JC, Cornsweet TN (1953) The disappearance of steadily fixated visual test objects. *J Opt Soc Am* 43:495–501.
3. Coppola D, Purves D (1996) The extraordinarily rapid disappearance of entopic images. *Proc Natl Acad Sci USA* 93:8001–8004.
4. Ratliff F, Riggs LA (1950) Involuntary motions of the eye during monocular fixation. *J Exp Psychol* 40:687–701.
5. Engbert R (2006) Microsaccades: A microcosm for research on oculomotor control, attention, and visual perception. *Prog Brain Res* 154:177–192.
6. Martinez-Conde S, Macknik SL, Hubel DH (2004) The role of fixational eye movements in visual perception. *Nat Rev Neurosci* 5:229–240.
7. Engbert R (2006) Flick-induced flips in perception. *Neuron* 49:168–170.
8. Martinez-Conde S, Macknik SL, Troncoso XG, Hubel DH (2009) Microsaccades: A neurophysiological analysis. *Trends Neurosci* 32:463–475.
9. Zuber BL, Stark L (1965) Microsaccades and the velocity-amplitude relationship for saccadic eye movements. *Science* 150:1459–1460.
10. Steinman RM, Haddad GM, Skavenski AA, Wyman D (1973) Miniature eye movement. *Science* 181:810–819.
11. Ditchburn RW (1980) The function of small saccades. *Vision Res* 20:271–272.
12. Kowler E, Steinman RM (1980) Small saccades serve no useful purpose: Reply to a letter by R. W. Ditchburn. *Vision Res* 20:273–276.
13. Rolfs M (2009) Microsaccades: Small steps on a long way. *Vision Res* 49:2415–2441.
14. Martinez-Conde S, Macknik SL, Hubel DH (2000) Microsaccadic eye movements and firing of single cells in the striate cortex of macaque monkeys. *Nat Neurosci* 3: 251–258.
15. Martinez-Conde S, Macknik SL, Hubel DH (2002) The function of bursts of spikes during visual fixation in the awake primate lateral geniculate nucleus and primary visual cortex. *Proc Natl Acad Sci USA* 99:13920–13925.
16. Kagan I, Gur M, Snodderley MD (2008) Saccades and drifts differentially modulate neuronal activity in V1: Effects of retinal image motion, position, and extraretinal influences. *J Vis* 8(14):19.1–25.
17. Leopold DA, Logothetis NK (1998) Microsaccades differentially modulate neural activity in the striate and extrastriate visual cortex. *Exp Brain Res* 123:341–345.
18. Bair W, O'Keefe LP (1998) The influence of fixational eye movements on the response of neurons in area MT of the macaque. *Vis Neurosci* 15:779–786.
19. Hafed ZM, Clark JJ (2002) Microsaccades as an overt measure of covert attention shifts. *Vision Res* 42:2533–2545.
20. Engbert R, Kliegl R (2003) Microsaccades uncover the orientation of covert attention. *Vision Res* 43:1035–1045.
21. Martinez-Conde S, Macknik SL, Troncoso XG, Dyar TA (2006) Microsaccades counteract visual fading during fixation. *Neuron* 49:297–305.
22. Rucci M, Iovin R, Poletti M, Santini F (2007) Miniature eye movements enhance fine spatial detail. *Nature* 447:851–854.
23. Ko HK, Poletti M, Rucci M (2010) Microsaccades precisely relocate gaze in a high visual acuity task. *Nat Neurosci* 13:1549–1553.
24. Troncoso XG, Macknik SL, Martinez-Conde S (2008) Microsaccades counteract perceptual filling-in. *J Vis* 8(14):15.1–9.
25. Poletti M, Rucci M (2010) Eye movements under various conditions of image fading. *J Vis* 10(3):6.1–18.
26. Collewijn H, Kowler E (2008) The significance of microsaccades for vision and oculomotor control. *J Vis* 8(14):20.1–21.
27. Rolfs M, Kliegl R, Engbert R (2008) Toward a model of microsaccade generation: The case of microsaccadic inhibition. *J Vis* 8(11):5.1–23.
28. Otero-Millan J, Troncoso XG, Macknik SL, Serrano-Pedraza I, Martinez-Conde S (2008) Saccades and microsaccades during visual fixation, exploration, and search: Foundations for a common saccadic generator. *J Vis* 8(14):21.1–18.
29. Engbert R, Mergenthaler K (2006) Microsaccades are triggered by low retinal image slip. *Proc Natl Acad Sci USA* 103:7192–7197.
30. Mergenthaler K, Engbert R (2010) Microsaccades are different from saccades in scene perception. *Exp Brain Res* 203:753–757.
31. Rucci M, Casile A (2004) Decorrelation of neural activity during fixational instability: Possible implications for the refinement of V1 receptive fields. *Vis Neurosci* 21: 725–738.
32. Pitkow X, Sompolinsky H, Meister M (2007) A neural computation for visual acuity in the presence of eye movements. *PLoS Biol* 5:e331.
33. Burak Y, Rokni U, Meister M, Sompolinsky H (2010) Bayesian model of dynamic image stabilization in the visual system. *Proc Natl Acad Sci USA* 107:19525–19530.
34. Engbert R, Kliegl R (2004) Microsaccades keep the eyes' balance during fixation. *Psychol Sci* 15:431–436.
35. Liang JR, et al. (2005) Scaling of horizontal and vertical fixational eye movements. *Phys Rev E Stat Nonlin Soft Matter Phys* 71:031909.
36. Mergenthaler K, Engbert R (2007) Modeling the control of fixational eye movements with neurophysiological delays. *Phys Rev Lett* 98:138104.
37. Freund H, Grassberger P (1992) The red queen's walk. *Physica A* 190:218–237.
38. Wyatt HJ (2010) The human pupil and the use of video-based eyetrackers. *Vision Res* 50:1982–1988.
39. Ciuffreda KJ, Tannen BW (1995) *Eye Movement Basics for the Clinician* (Mosby, St. Louis).
40. Carpenter RH (2000) The neural control of looking. *Curr Biol* 10:R291–R293.
41. Sparks DL (2002) The brainstem control of saccadic eye movements. *Nat Rev Neurosci* 3:952–964.
42. Hafed ZM, Goffart L, Krauzlis RJ (2009) A neural mechanism for microsaccade generation in the primate superior colliculus. *Science* 323:940–943.
43. Collins JJ, De Luca CJ (1993) Open-loop and closed-loop control of posture: A random-walk analysis of center-of-pressure trajectories. *Exp Brain Res* 95:308–318.
44. Ölveczky BP, Baccus SA, Meister M (2003) Segregation of object and background motion in the retina. *Nature* 423:401–408.

Supporting Information

Engbert et al. 10.1073/pnas.1102730108

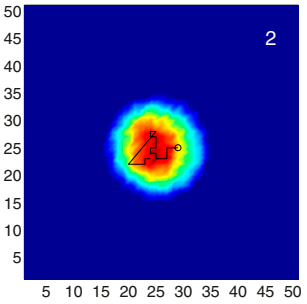

Movie S1. Animation of 1,000 iterations of the self-avoiding random walk model. The eye's trajectory is indicated by the thin black line. The activation field is indicated by the color coding (with increasing activation from dark blue to red). During the simulation of the model, 19 microsaccades are triggered by critical activations (see the counter at the top right part of the animation). Model parameters are given in the main text. Note that the potential is not visualized.

Movie S1